PHYSICAL REVIEW B VOLUME 13, NUMBER 12 15 JUNE 1976

# Possibility of adsorbate position determination using final-state interference effects

P. A. Lee
*Bell Laboratories, Murray Hill, New Jersey 07974*
(Received 30 December 1975)

Novel methods for the determination of adsorbate position on surfaces based on final-state interference effects are discussed. The first is the measurement of extended x-ray absorption fine structure (EXAFS) from excitation of the adsorbed atom by monitoring the intensity of the Auger emission line as a function of photon energy. Such an experiment should be feasible with synchrotron radiation. The sensitivity of surface EXAFS to adatom position is demonstrated by calculations appropriate for adsorption of Se on several crystal faces of Ni. We also examine the possibility of measuring EXAFS by monitoring the photoelectron intensity and conclude that an average over a hemisphere outside the crystal is not sufficient to reduce the photoemission data to EXAFS. Relations between EXAFS and angular-resolved photoemission are elucidated and it is shown that the single scattering EXAFS theory includes second-order scattering from the excited atom in photoemission theory.

## I. INTRODUCTION

Recently there has been a revival of interest in extended x-ray absorption fine structure (EXAFS). Considerable amount of work has been stimulated by the suggestion of Sayers, Stern, and Lytle[1] that EXAFS may provide a new tool for structural determination in situations where conventional x-ray diffraction fails. Experimentally the field has undergone major advances with the availability of synchrotron radiation.[2] The greatly increased intensity means that spectra that used to take weeks can now be obtained in minutes. The availability of the new x-ray source naturally leads one to consider new classes of experiments that were previously impossible. In particular, a number of people have recognized that EXAFS may provide a new method for structural determination of surfaces with adsorbed atoms. EXAFS has the obvious advantage that it is sensitive to the local environment of a particular species of atom. Thus in principle one can tune in on the adsorbed atom and deduce its position relative to the substrate by determining its distances to a set of neighbors. Unlike low-energy electron diffraction (LEED) the adsorbed atoms are not required to form a periodic array. Furthermore, it has been shown[3] that, by and large, multiple scattering effects average out in EXAFS and relatively simple single scattering theory gives satisfactory results.[3,4] The obvious difficulty is that the absorption by one monolayer of atoms is so small that EXAFS from the adsorbate will not show up in the intensity of the transmitted x ray. To get around that difficulty, and the more general problem of weak absorption by dilute systems, EXAFS measurements have recently been performed[5] in which the absorption coefficient is measured by monitoring the fluorescence from the atoms that have absorbed the x ray. However, application of this technique to an adsorbed layer will most likely be limited to heavy adsorbates on light substrates; otherwise the signal will be dominated by the background radiations from the bulk. A closely related method which we suggest here is to monitor the absorption coefficient by measuring the Auger electron intensity. The $K$ shell is filled by a $KLL$ Auger process with a probability of ~30% in copper and even higher in lighter atoms. The resulting Auger electron has a well-defined energy and one can energy analyze the electrons with crude resolution ($\gtrsim 2$ eV) to eliminate background electrons. Since energy resolution of electrons can be performed over a wide range of electron energy and the background electron can originate only from a few angstroms inside the surface, this method has an obvious advantage in terms of signal to background over fluorescence measurements in surface experiments. We should point out however, that this technique is generally not applicable to adsorbates from the first row in the Periodic Table (with the possible exception of Ne and partially ionized states of O and F) as the recombination in these cases involves valence-band electrons resulting in very broad Auger spectra. If we stay away from these few, albeit important cases, crude estimates based on available intensity from the Stanford Synchrotron Radiation Project indicate that this experiment is indeed feasible at the present time. To test the sensitivity of surface EXAFS to adsorbate position we have performed calculations of the spectra expected for Se adsorbed on several faces of Ni. More sophisticated calculations than those presented here are possible but it is hoped that these results will encourage experimental work in this area.

Yet another possible alternative experiment is to measure the total number of photoelectrons that

have been elastically emitted. One might be tempted to think that the total yield must be proportional to the absorption coefficient. Indeed EXAFS have been measured using quantum yield over a 100-eV energy range on solid and liquid sodium by Peterson and Kunz.[6] In that case a high-pass filter is sufficient to suppress the background electrons. However, in our case we are interested in EXAFS from an adsorbate on a single crystal surface. Experimentally, the largest solid angle into which photoelectrons can be collected is only $2\pi$ sr. The intrinsic asymmetry of the position of the adsorbate relative to the scatterers raises doubt that a $2\pi$-solid-angle averaged measurement of the electron yield is proportional to the total absorption. To answer this question, we are led to study the angular distribution of photoelectron emission from an adsorbed atom. As we shall see, our conclusion is that a $2\pi$ sr average of the photoelectron yield is not proportional to EXAFS.

The problem of final-state effects on electron emission from localized sources has, just as in the case of EXAFS, a long history. Experimentally, unusual diffraction patterns were first observed by Kikuchi[7] in electron diffraction experiments and were explained by von Laue[8] as being due to final-state interference of secondary electron emission. The localized emission sources may be electrons excited directly from core states or Auger electrons, depending on the excitation mechanism. Recently, Liebsch[9] has suggested that angular resolved photoemission may be a tool for determination of adsorbate geometry and McDonnel, Woodruff, and Holland[10] have measured the angular distribution of Auger electrons and have emphasized its sensitivity to adsorbate position. In his analysis Liebsch utilizes the translational periodicity parallel to the surface. His analysis is very close in spirit to LEED calculations. That the sophisticated theoretical machinery devised for LEED may readily be adapted to this problem was recently emphasized by Pendry[11] and by Holland.[12] This point was recognized in Liebsch's original article[9] and very recently Liebsch has performed numerical calculations appropriate for sulphur adsorbed on nickel.[13] We have formulated a "short-range-order theory" for the photoemission angular distribution which is closer in spirit to EXAFS theory. Relations between this and EXAFS and Liebsch's formulations will be elucidated and the practical importance of studying photoemission normal to the surface will be examined.

## II. SURFACE EXAFS

We begin with a brief review of EXAFS. EXAFS refers to the modulation of the absorption spectrum which is readily observed up to 1000 eV above the threshold. Such modulation arises because the final state of the photoelectron is perturbed by the surrounding atoms. A convenient way to visualize this perturbation is to picture the electron as propagating outwards and then being backscattered by its neighbors. The backscattered wave contributes to the final-state wave function with a phase difference given by $2kr_j$, where $k$ is the photoelectron momentum and $r_j$ is the distance to the neighbor. In addition the phase shift suffered during the scattering and the phase shift due to motion through the central atom potential must be taken into account. The above picture yields the following formula for the modulation of the absorption coefficient normalized to the unperturbed value:

$$\chi = \frac{\delta\alpha}{\alpha_0} = \sum_{mLL''} 4\pi \langle L_0|\hat{\epsilon}\cdot\vec{r}|L''\rangle Y^*_{L''}(-\hat{r}_j) Y_L(\hat{r}_j)\langle L|\hat{\epsilon}\cdot\vec{r}|L_0\rangle \left(\sum_{m_0}\sum_{L}|\langle L_0|\hat{\epsilon}\cdot\vec{r}|L\rangle|^2\right)^{-1}$$

$$\times \sin[2kr_j + \delta'_L(k) + \delta'_{L''}(k) + \Psi(k)]\,|f(\pi)|\,e^{-2\gamma r_j}\,\frac{e^{-2\sigma_j^2 k^2}}{kr_j^2}\,. \tag{2.1}$$

In words this equation describes the excitations of a level $L_0 = (l_0, m_0)$ to a state with angular momentum $L$ which propagates in the direction $\hat{r}_j$ with probability amplitude $Y_L(\hat{r}_j)$. It is backscattered by the atom with amplitude $|f(\pi)|e^{i\Psi(k)}$. The reflected wave has an angular component $L''$ as it propagates towards the central atom according to $Y^*_{L''}(-\hat{r}_j)$ and is connected back to $L_0$ by the dipole matrix element. The central atom phase shifts $\delta'_L$ and $\delta'_{L''}$ describes the propagation of the outgoing and incoming wave in the central atom potential. An exponential damping factor $e^{-2\gamma r_j}$ has been included to account for losses due to inelastic scattering and a Debye-Waller factor $e^{-2\sigma_j^2 k^2}$ to account for atomic vibration. A number of simplifying assumptions have been made in arriving at Eq. (2.1). One assumption is that the spherical outgoing wave can be treated as a plane wave as

far as the scattering by the neighboring atom is concerned. It has been possible to relax this assumption[3] resulting in an effective $|f(\pi)|$ and $\Psi(k)$ which then depends on $r_j$. Such corrections are found to be small at moderate energy and will be ignored in this paper. Equation (2.1) also does not include multiple scattering effects, but we argue that this neglect is not serious. It has been found possible to include multiple scattering by adding up all possible paths for the photoelectron.[3] Clearly the phase difference is $kr_{\text{tot}}$ instead of $2kr_j$, where $r_{\text{tot}}$ is the total path length. These path lengths are generally quite large compared with near neighbor spacing and give rise to rapidly oscillating contribution to $\chi$ which tend to average out. This has been demonstrated by explicit calculation for the case of copper metal.[3] Except for unusual situations like the fourth shell, which is directly shadowed by the first shell, multiple scattering is found to be a small correction. This kind of argument does not work for LEED because in that case the path difference between a double scattering in the first layer and a single scattering by the second layer can be arbitrary. Furthermore, in EXAFS the electron is produced and detected at the same point and as a result, most paths must undergo several large-angle scatterings in order to return to the origin and such scattering amplitudes are small.

We now specialize to the case of excitation of an $s$ state. The angular part of the matrix elements is very simple and Eq. (2.1) becomes

$$\chi = -\sum_j \frac{3\cos^2\theta_j}{kr_j^2} \sin[2kr_j + 2\delta_1'(k) + \Psi(k)] \times |f(\pi)|^{-2\gamma r_j} e^{-2\sigma_j^2 k^2}, \quad (2.2)$$

where $\theta_j$ is the angle between $\vec{r}_j$ and the polarization direction $\hat{\epsilon}$. For polycrystalline sample $3\cos^2\theta_j$ averages out to unity and we recover the usual result.[1] The computations in the rest of the paper will be based upon Eq. (2.2). As a check we have applied the computation to copper metal. The result is very similar to the simple scattering theory performed by Lee and Pendry[3] and compares rather well with experiment.

To demonstrate the sensitivity of surface EXAFS to adsorbate position and to estimate the magnitude of the effect, we have performed calculations using Eq. (2.2) with parameters which would approximate the adsorption of Se on Ni. The inputs are the Ni phase shifts and the central atom phase shift $\delta_1'$ for Se. (In fact, the Hartree-Fock phase shift using a program by Pendry[14] for copper has been used. The difference between copper and nickel phase shifts is the same order as the difference between Hartree-Fock and $X\alpha$ calculations.[15] Elsewhere[16] we have pointed out that the central atom phase shift for Se should be approximated by the ionized bromine phase shift to account for relaxation. Here we have simply used the bromine atom phase shift. Again the difference is small, ~0.2 rad. These points can clearly be refined as data become available.) It is worthwhile to point out that substituting lighter atoms like oxygen or sulfur will modify only $\delta_1'(k)$. The magnitude of the EXAFS oscillations is determined only by the substrate. We have also used an energy-dependent damping $\gamma = 0.147/k$ (in atomic units) which corresponds to an imaginary part of the self-energy of 4 eV, a number obtained from LEED experiments. It is possible that for atoms in the first layer there should be much less damping. These effects can be easily incorporated in the future. For simplicity we have not included backscattering from other adatoms and have also omitted the Debye-Waller factor.

The LEED experiments[17] suggest that the nearest-neighbor Se-Ni distance is close to a bond length of 2.27 Å. We have chosen the adatom position to satisfy this bond length and have then moved the adatom 0.2 a.u. or ~0.1 Å in and out of the surface plane. Figure 1 shows the expected EXAFS from an atom adsorbed in the fourfold hollow in the (001) plane for these three vertical positions. Note that relative peak heights change and peak positions move systematically. As discussed earlier and demonstrated by explicit calculations for copper,[3] multiple scattering corrections do not produce changes and systematic shifts that correspond to those indicated in Fig. 1 by varying the distances. However, to make absolute distance determination reliable central atom

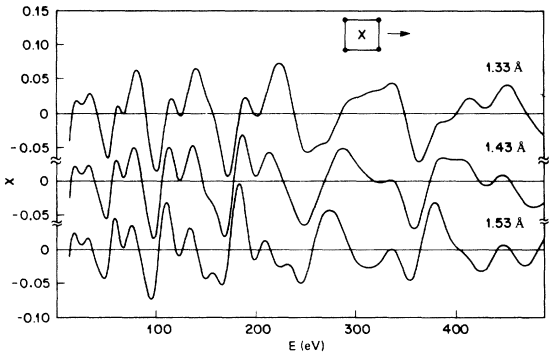


FIG. 1. Theoretical EXAFS spectrum for Se adsorbed on the (001) surface of nickel. The Se atom is assumed to be in the fourfold hollow and the distance from the last atomic plane is indicated for each curve. Polarization is in the surface plane and in the direction indicated. Debye-Waller factors have not been included in these plots.

phase shifts $\delta_l'(k)$ are required. The phase shifts can be determined from model systems with known distances and recent work on simple molecules shows[18] that such measured phase shifts can be used to predict distances in simple molecules to within 0.02 Å. Furthermore recent development[19] in the calculation of such phase shifts indicates that much better agreement in absolute distance determination than the 0.1 Å obtained for copper using Hartree-Fock phase shifts[3] is possible. Thus our knowledge of the phase shifts is sufficient to distinguish changes shown in Fig. 1. Furthermore if good quality data is obtained over a sufficiently wide energy range it should be possible to obtain distances by Fourier-transform techniques. This is especially true for the nearest-neighbor distance which is well separated from other distances. It has been shown in many cases[1] that this distance can be obtained to better than 0.1 Å when the shift is calibrated using known materials as standards.

A more interesting situation is the (110) surface. The substrate is made up of rectangular cells and it is found that whereas sulfur on nickel sits in the hollow, oxygen on nickel sits in a bridge position over the short side of the rectangle.[20] In Figs. 2 and 3 we compare the difference between those two sites. Even for the same nearest-neighbor distances the contrast is striking.

Synchrotron radiation is linearly polarized and in Fig. 4 we compare two different polarization directions (both in the surface plane) for the hollow position. Again the change is substantial. Such changes can be used as further checks on the position assignment.

In Fig. 5 we show some calculations for the most unfavorable case. In the (111) direction there are two alternate sites in the threefold hollow, one of which has an atom directly underneath

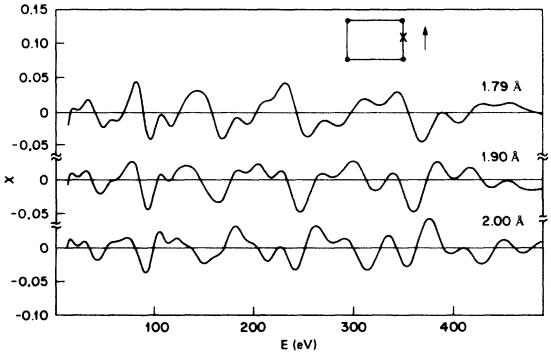


FIG. 2. (110) surface of nickel with Se atom in the short bridge position. Polarization is in the surface plane.

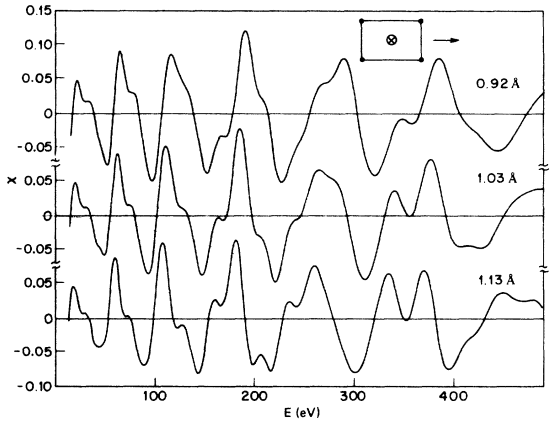


FIG. 3. (110) surface of nickel with Se atom in the center of the rectangle. The nearest neighbor is immediately below the adatom. Polarization is in the surface plane.

the adatom in the second layer. It turns out that the first-, second-, and fourth-neighbor structures are the same in both cases. We have compared the two sites with a polarization vector that makes a 45° angle with the plane to gain some sensitivity to the third-nearest neighbor. The difference between the two sites is probably at the limit of our confidence in the simple theory. It may still be possible to resolve the difference by Fourier transform if high-quality data is available, or by polarization effects since the orientation of the nearest-neighbor triangle is different for the two sites.

Finally we comment on whether the calculated amplitude for the EXAFS oscillations are realistic. When compared with EXAFS measured by transmission it has been found that the theory is too large by about 50%.[2,3] Recently we have proposed[16] that this discrepancy is due to the fact that only the elastic electron contributes to the EXAFS and its relative strength is estimated to be 70%

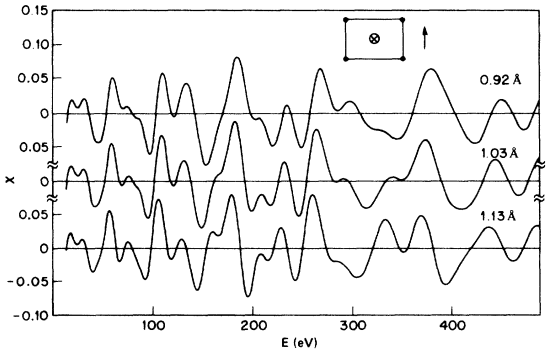


FIG. 4. (110) surface of nickel with polarization in the surface plane but pointing in a different direction from that in Fig. 3.

of the total number of emitted photoelectrons. However, if EXAFS is measured by Auger electron spectroscopy, the Auger electrons emitted from atoms that have undergone shakeup or shakeoff processes will presumably be shifted in energy and be removed from the primary peak being monitored. Thus, the modulation in the intensity of the primary Auger line should not require the 70% correction and the calculations shown here should approximate more closely the experimental measurement.

## III. RELATION TO ANGULAR RESOLVED PHOTOEMISSION FROM ABSORBATE

We now turn our attention to the problem of measuring surface EXAFS by monitoring the intensity of the photoelectrons. The angular distribution of photoelectrons from absorbates has been studied by Liebsch.[9] His approach is similar in spirit to LEED in that he makes use of the translational symmetry in the surface plane. To make contact with EXAFS we would like to recast his formulation into a "short-range-order theory" in which we consider scattering by each individual atom. If the electron mean free path is short this later approach is more convenient. This is indeed the case for EXAFS. The main conclusion we draw from this section is that the simple EXAFS expression is the result of intricate cancellations upon a $4\pi$ sr averaging of the angular resolved photoemission expression. Consequently a measurement of the photoelectron emitted into a hemisphere outside the crystal will not be the same as EXAFS. We also elucidate the origin of the central atom phase shift term in the EXAFS expression and show that the single scattering expression for EXAFS actually includes second-order scattering processes in angular resolved photoemission.

We calculate the photoemission into a particular angle $\hat{k}$ by the golden rule. Note that in EXAFS

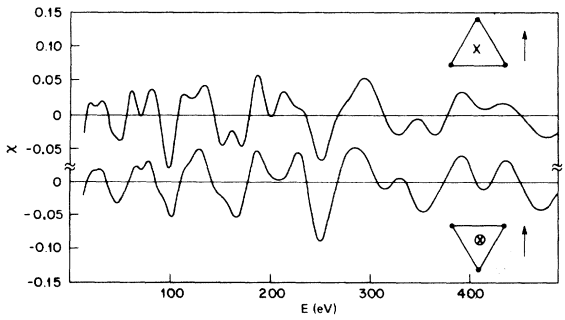


FIG. 5. (111) surface of nickel with Se occupying two inequivalent sites. Polarization makes a 45° angle with the surface plane.

the total absorption rate is given by

$$\alpha \sim \sum_f |\langle i|\hat{\epsilon}\cdot\vec{r}|f\rangle|^2 \delta(\omega-\epsilon_f-\epsilon_i)\,, \tag{3.1}$$

and $|f\rangle$ is any complete set of eigenstate of the Hamiltonian. However, we are now interested in the emission probability in a given direction $\hat{k}$ and we must choose the final state with some care. Let us consider the problem of a single neighbor located at $\vec{r}_j$ relative to the excited atom, ignoring for the moment the potential due to the excited atom. The eigenstates of this problem can be written down exactly in terms of the $T$ matrix and consists of an unperturbed plane wave $|\vec{k}\rangle$ plus a scattered wave:

$$|f\rangle = |\vec{k}\rangle + G_0^- T^- |\vec{k}\rangle\,, \tag{3.2}$$

where

$$G_0^\pm = (\tfrac{1}{2}k^2 - H_0 \pm i\delta)^{-1}\,, \tag{3.3}$$

and

$$T^\pm = V + V G_0^\pm T^\pm \tag{3.4}$$

is the $T$ matrix due to the atomic potential $V$ of the scatterer. Equation (3.2) is equivalent to the Lipmann-Schwinger equation.[21] Note that by choosing $G_0^- T^-$ in Eq. (3.2) we have chosen a solution corresponding to a plane wave plus incoming spherical waves. This is in fact the appropriate final state for measurement of photoemission in the $\hat{k}$ direction as a plane wave plus outgoing waves would imply probability of emission in all other directions as well. This point has been discussed in detail by Breit and Bethe.[22] The emission rate $P(\hat{k})$ is then given by

$$P(\hat{k}) = D|\langle i|\hat{\epsilon}\cdot\vec{r}|f\rangle|^2\,, \tag{3.5}$$

where the state $|f\rangle$ is given by Eq. (3.2). In Eq. (3.5) it is understood that the magnitude of $\vec{k}$ is determined by energy conservation and $D$ is a slowly varying factor that includes the density of states. For simplicity we shall specialize to the case where $|i\rangle$ is an $s$ state. Putting Eq. (3.2) into (3.5) we can write

$$P(\hat{k}) = D\left| M(\hat{\epsilon}\cdot\hat{k}) + \langle\vec{k}|\sum_j T_j^+ G_0^+(k)\hat{\epsilon}\cdot\vec{r}\,|i\rangle\right|^2\,, \tag{3.6}$$

where

$$M = (4\pi)^{1/2}\int_0^\infty dr\, r^3(-i)j_1(kr)\Phi_i(r)\,, \tag{3.7}$$

is the matrix element with the core-state radial wave function $\Phi_i(r)$.

We shall need several representations of the Green's function[21]:

$$G_0^+(k,\vec{r},\vec{r}') = \sum_{\vec{k}'} \frac{e^{i\vec{k}'\cdot(\vec{r}-\vec{r}')}}{k^2/2 - k'^2/2 + i\delta}, \tag{3.8}$$

$$G_0^+(k,\vec{r},\vec{r}') = e^{ik|\vec{r}-\vec{r}'|}/2\pi|\vec{r}-\vec{r}'|, \tag{3.9}$$

$$G_0^+(k,\vec{r},\vec{r}') = -2ik\sum_L j_l(kr_<)h_l^{(1)}(kr_>) \times Y_L(\hat{r})Y_L^*(\hat{r}'). \tag{3.10}$$

The last form is obtained from the first by expanding $e^{i\vec{k}\cdot\vec{r}}$ in spherical harmonics and then performing the $k^2\,dk$ integral by contour integration after extending the integral to negative $k$ using the symmetry properties of $j_l$. Using Eq. (3.10) we can write

$$\langle\vec{k}|T_j^+G^+\hat{\epsilon}\cdot\vec{r}|i\rangle = -\frac{Mk}{2\pi}\int d\vec{r}\,d\vec{r}'\,e^{-i\vec{k}\cdot\vec{r}'} \times T(\vec{r}'-\vec{r}_j,\vec{r}-\vec{r}_j)h_1^{(1)}(kr)\hat{\epsilon}\cdot\hat{r}. \tag{3.11}$$

We note that $T(\vec{r}',\vec{r})$ is nonzero only near $\vec{r}=\vec{r}'\approx\vec{r}_j$. For $kr_j \gg 1$ we approximate

$$-ih_1^{(1)}(kr)\hat{\epsilon}\cdot\hat{r} \approx i(e^{ikr}/kr)\hat{\epsilon}\cdot\hat{r} \approx i(e^{i\vec{k}_j\cdot\vec{r}}/kr_j)\hat{\epsilon}\cdot\hat{r}_j, \tag{3.12}$$

where $\vec{k}_j = k\hat{r}_j$. We have made the assumption that the spherical wave can be approximated by a plane wave propagating in the $\hat{r}_j$ direction by the time it reaches the scatterer. Now the $\vec{r}$ and $\vec{r}'$ integrals can be performed and Eq. (3.11) becomes

$$\langle\vec{k}|T_j^+G^+\hat{\epsilon}\cdot\vec{r}|i\rangle = -\frac{M}{2\pi}\frac{e^{i(\vec{k}_j-\vec{k})\cdot\vec{r}_j}}{r_j}T(\vec{k},\vec{k}_j)\hat{\epsilon}\cdot\hat{r}_j, \tag{3.13}$$

where $T(\vec{k},\vec{k}_j)$ is the Fourier transform of $T(\vec{r}',\vec{r})$. When $|\vec{k}| = |\vec{k}_j|$

$$T(\vec{k},\vec{k}_j) = -2\pi f(\theta_j),$$

where $\theta_j$ is the angle between $\vec{k}$ and $\vec{r}_j$, i.e., $\cos\theta_j = \hat{k}\cdot\hat{r}_j$. Using these simplifications, Eq. (3.13) can be put into Eq. (3.6) and we obtain

$$P(\hat{k}) = D|M|^2\left|\hat{\epsilon}\cdot\hat{k} + \sum_j \frac{f(\theta_j)}{r_j}\,e^{ikr_j(1-\cos\theta_j)}\hat{\epsilon}\cdot\hat{r}_j\right|^2. \tag{3.14}$$

The cross term is the interference term which exhibits oscillations with variation in $k$. Equation (3.14) is not new[23] and McDonnel *et al.*[10] have performed calculations for the angular distribution of Auger electrons using a similar formulation. Equation (3.14) has the simple interpretation of interference between the plane wave $|\vec{k}\rangle$ with the wave which propagates towards $\vec{r}_j$ and is then scattered in the $\vec{k}$ direction with amplitude $f(\theta_j)$. The phase factor $kr_j(1-\cos\theta_j)$ is simply related to the difference in the two path lengths. We presented the derivation in some detail because later we want to generalize Eq. (3.14) to include the effect of the excited atom potential.

Formally we know that the integration of $P(\hat{k})$ over all solid angle $\hat{k}$ must yield the total absorption rate which we have seen is proportional to

$$1 - 2\sum_j \mathrm{Im}[f(\pi)e^{2ikr_j}]/kr_j^2$$

to first order in the scattering amplitude. That this is indeed the case can be shown explicitly from Eq. (3.14). Let us focus our attention on the cross term

$$\int\frac{d\hat{k}}{4\pi}P^{(1)}(\hat{k}) = D|M|^2\,2\,\mathrm{Re}\left(\sum_j e^{ikr_j}\hat{\epsilon}\cdot\hat{r}_j\frac{I_j}{r_j}\right), \tag{3.15}$$

where

$$I_j = \int\frac{d\hat{k}}{4\pi}\hat{\epsilon}\cdot\hat{k}e^{-ikr_j\cos\theta_j}f(\theta_j). \tag{3.16}$$

This integral can be performed by choosing $\hat{r}_j$ as the $\hat{z}$ axis and writing

$$\hat{\epsilon}\cdot\hat{k} = \sum_m\left(\frac{4\pi}{3}\right)Y_{1m}^*(\hat{\epsilon})Y_{1m}(\hat{k}).$$

The azimuthal angle integration immediately yields $m=0$ and the integral is reduced to

$$I_j = \hat{\epsilon}\cdot\hat{r}_j\,\tfrac{1}{2}\int d\cos\theta_j\cos\theta_j\,e^{-ikr_j\cos\theta_j}f(\theta_j) = \hat{\epsilon}\cdot\hat{r}_j\sum_l i\frac{\partial}{\partial(kr_j)}[(-i)^l j_l(kr_j)]f_l. \tag{3.17}$$

In the second line we have expanded

$$f(\theta) = \sum_l f_l P_l(\cos\theta)$$

and $e^{-ikr_j\cos\theta}$ in $P_l(\cos\theta)$ in the standard way. Using the asymptotic form of $j_l(kr)$ we finally obtain

$$I_j = [(\hat{\epsilon}\cdot\hat{r}_j)/kr_j]\tfrac{1}{2}i[f(\pi)e^{ikr} + f(0)e^{-ikr}]. \tag{3.18}$$

Equation (3.15) then becomes

$$\int\frac{d\hat{k}}{4\pi}P^{(1)}(\hat{k}) = -\sum_j\frac{(\hat{\epsilon}\cdot\hat{r}_j)^2}{kr_j^2}\mathrm{Im}[e^{2ikr_j}f(\pi) + f(0)]. \tag{3.19}$$

Noting that the $(\hat{\epsilon}\cdot\hat{k})^2$ term in Eq. (3.14) averages out to be $\frac{1}{3}$ we see that the oscillatory part compared with the unperturbed part is precisely the EXAFS expression with central atom phase shift $\delta_1'$ set equal to zero. The part proportional to $f(0)$ is nonoscillating and arises from the incoming part of the plane wave. This part does not con-

tribute to EXAFS and indeed it is exactly cancelled by the angular average of the modulus of the second term in Eq. (3.14) arising from the same atom. This is easily shown by use of the optical theorem,

$$\mathrm{Im}f(0)=\frac{k}{4\pi}\int d\varphi\, d\cos\theta\,|f(\theta)|^2. \tag{3.20}$$

That this cancellation has to take place can be shown more generally by working with Eq. (3.6) and using the formal expression[21]

$$\mathrm{Im}T=\tfrac{1}{2}iT^-(G^+-G^-)T^+, \tag{3.21}$$

while we have not demonstrated it explicitly, it must be true that a similar cancellation occurs between the angular average of the squared term arising from different atoms, i.e., terms of the form

$$f(\theta_i)f^*(\theta_j)e^{ikr_i(1-\cos\theta_i)}e^{-ikr_j(1-\cos\theta_j)},\quad i\neq j,$$

and the angular average of the second-order scattering term from atoms $i$ and $j$. This is because in EXAFS we know that multiple scattering involves sums of interatomic distances, and not their differences.

From Eq. (3.4) we see that for each particular $\hat{k}$ direction the oscillatory term is not at all like the EXAFS oscillation. The period $2r_j$ is replaced by $r_j(1-\cos\theta_j)$. It is only by integrating over $4\pi$ that we recover the EXAFS result. It is then obvious that integrating over a hemisphere is not sufficient to reproduce the EXAFS result. While it is true that quantum yield measurement is found to compare well with EXAFS,[6] in that case the excited atom can be anywhere within the escape depth of the surface. Furthermore, the surface is polycrystalline. These factors may be sufficient to make the measured quantum yield effectively a $4\pi$ average.

We next consider the inclusion of inelastic effects. In EXAFS the excited atom is in the bulk and a simple model is to add an imaginary part to the photoelectron energy, i.e., $E=\frac{1}{2}k^2$ is replaced by $E+i\Gamma$. The above discussion still holds if the $\vec{k}$ vector is generalized to represent a complex quantity defined by $\vec{k}=(k_0+i\gamma)\hat{k}$, where $k_0$ and $\gamma$ are the real and imaginary part of $(2E+2i\Gamma)^{1/2}$. Then integration of $P(\hat{k})$ over any finite sphere will be proportional to the EXAFS expression. However, for adsorbed atoms we have to consider a model in which damping occurs only in half space for negative $z$. In this case the noninteracting eigenstates are given by

$$\langle\vec{r}\,|\vec{k}\rangle=\begin{cases}e^{i\vec{k}\cdot\vec{r}-\gamma_z r_z}, & r_z<0,\\ e^{i\vec{k}\cdot\vec{r}}, & r_z>0,\end{cases}$$

and

$$\langle\vec{k}\,|\vec{r}\rangle=\begin{cases}e^{-i\vec{k}\cdot\vec{r}-\gamma_z r_z}, & r_z<0,\\ e^{-i\vec{k}\cdot\vec{r}}, & r_z>0,\end{cases} \tag{3.22}$$

where

$$\gamma_z=\mathrm{Im}(2E-k_\parallel^2+i2\Gamma)^{1/2}, \tag{3.23}$$

and $k_\parallel$ is the component of $\vec{k}$ parallel to the surface. In Eq. (3.22) only damping in the $z$ direction is chosen because that is the only solution that matches a plane wave at the surface. Note that the right-hand eigenstate $|\vec{k}\rangle$ is not the complex conjugate of the left-hand eigenstate $\langle\vec{k}|$ because the Hamiltonian is not Hermitian. It is interesting to note that inside the substrate the amount of damping described by Eq. (3.22) is the same as that described by a complex $\vec{k}$ vector because, to first order in $\Gamma$, $\gamma r=\gamma_z z$ for a wave that propagates a distance $r$ in the $\hat{k}$ direction. Thus we should generalize Eq. (3.14) by including a damping factor in the second term given by $e^{-\gamma r_j+\gamma_z\vec{r}_j\cdot\hat{z}}$, where $\hat{r}_j\cdot\hat{z}<0$.

Our next step is to make contact with Liebsch's theory. It is derived by using the plane-wave representation Eq. (3.8) for $G^+$ instead of the spherical wave representation. Let us follow Liebsch and consider a semi-infinite cubic structure such that $\vec{r}_j=n\hat{x}+m\hat{y}+p\hat{z}$, where $n,m=-\infty$ to $\infty$ and $p=-\infty$ to 0. We denote the adsorbate position as $\vec{r}_a$. Then

$$\sum_j\langle k|T_j^\dagger G^+\hat{\epsilon}\cdot\vec{r}\,|i\rangle = \sum_{j\vec{k}'}\frac{T(\vec{k},\vec{k}')2e^{i(\vec{k}'-\vec{k})\cdot\vec{r}_j}}{k^2-k'^2+i\delta}\hat{\epsilon}\cdot\hat{k}'M. \tag{3.24}$$

The sum over $n,m$ results in $\delta^2(\vec{k}'_\parallel-\vec{k}'_\parallel+\vec{G}_\parallel)$ where $\vec{G}_\parallel$ are reciprocal-lattice vectors in the plane. Note that this remains so even with damping as damping affects only the $k_z$ component. The $k_z$ integral is performed next yielding $\delta(k'_z+(2E+2i\Gamma-k'^2_\parallel)^{1/2})$. [One argues that $T(\vec{r},\vec{r}')$ is localized within the muffin-tin radius $r_m$, and hence the singularity structure is dominated by the $e^{ik_z r_{jz}}$ term if $|r_{jz}|>r_m$.] This $\delta$ function places the intermediate state $\vec{k}'$ on the energy shell and points it towards the substrate. The $p$ sum is then performed, giving $(1-e^{ik'_z a})^{-1}$, where $a$ is the lattice constant. One then obtains

$$\sum_j\langle\vec{k}\,|T_j^\dagger G^+\hat{\epsilon}\cdot\hat{r}|\,i\rangle = \sum_{G_\parallel}M\hat{\epsilon}\cdot\hat{k}f(\theta_{\vec{k}\vec{k}'})\frac{i}{k'_z}\frac{e^{i(\vec{k}'-\vec{k})\cdot\vec{r}_a}}{1-e^{ik'_z a}}, \tag{3.25}$$

where $\vec{k}'(\vec{G}_\parallel)$ is determined by the $\delta$ functions stated

above and $\theta_{\vec{k}\vec{k}'}$ is the angle between $\hat{k}$ and $\hat{k}'$. Thus we see that Liebsch's theory is mathematically equivalent to the short-range order theory given by Eq. (3.14).

The above derivation of the EXAFS expression by averaging the angular resolved photoemission result raises an apparent paradox. The potential of the central atom can be incorporated in the photoemission expression by inclusion of a phase shift. However, since the direct wave and scattered wave are both outgoing waves they are phase shifted by the same amount and the central atom phase shift will cancel out in the interference term. To this order the only effect of the central atom is to modify the matrix element $M$ and the central atom phase shift does not enter either the photoemission or the EXAFS expression. This point is evident from Eq. (3.1) of Liebsch's work.[13] It is then of interest to consider in some detail the role of the central atom potential and show explicitly where the central atom phase shift in EXAFS comes from.

We take the unperturbed Hamiltonians as $H_0' = p^2/2m + V_c(r)$ where $V_c(r)$ is the central atom potential. Our previous procedures must then be modified in two ways. First the unperturbed state $|\vec{k}\rangle$ is an eigenstate of $H_0'$. The eigenstates are well known in the scattering problem and can be chosen as a plane wave plus either an incoming or an outgoing wave. For reasons discussed earlier the appropriate choice is the incoming state, i.e., asymptotically

$$\langle \vec{r}|\vec{k}\rangle = \Phi_k^- = e^{i\vec{k}\cdot\vec{r}} + f_c^*(\pi-\theta)e^{-ikr}/r, \tag{3.26}$$

where $\theta$ is the angle between $\vec{k}$ and $\vec{r}$ and $f_c$ is the scattering amplitude due to the central atom. This is to be contrasted with the better known form

$$\Phi_k^+ = e^{i\vec{k}\cdot\vec{r}} + f_c(\theta)e^{ikr}/r. \tag{3.27}$$

A second modification is that we replace the free-particle Green's function $G_0^+$ by $G_c^+$ which satisfies the equation

$$G_c^+ = G_0^+ + G_0^+ V_c G_c^+. \tag{3.28}$$

An analogous representation to Eq. (3.10) is

$$G_c^+(k,\vec{r},\vec{r}') = -2ik\sum_L \Phi_l(k,r_<)h_l^{(1)}(kr_>)Y_L(\hat{r})Y_L^*(\hat{r}'), \tag{3.29}$$

provided $r_>$ is larger than the muffin-tin radius. Here $\Phi_l(k,r)$ is the regular solution of the Schrödinger equation which equals $e^{i\delta_l}(h_l^{(1)}e^{i\delta_l} + h_l^{(2)}e^{-i\delta_l})$ outside the muffin-tin radius.[24] Equation (3.29) is obtained by putting Eq. (3.10) into Eq. (3.28) and noting that $\Phi_l(kr)$ satisfies the equation

$$\Phi_l(kr) = j_l(kr) + \int j_l(kr_1)V_c(r_1)G_c^+(l,r,r_1)r_1^2 dr_1. \tag{3.30}$$

We then proceed exactly as before, the only change being that the matrix element $M$ is now between the initial-state and the exact radial solution inside the muffin-tin radius. An important additional term arises however, since the state $|\vec{k}\rangle$ in Eq. (3.11) is no longer a plane wave, but has the additional incoming wave. We approximate the incoming spherical wave by a plane wave as before

$$\begin{aligned} f_c^*(\pi-\theta)e^{-ikr}/r &\approx f_c^*(\pi-\theta)e^{-i\vec{k}_i\cdot\vec{r}}/r \\ &\approx f_c^*(\pi-\theta)e^{-i\vec{k}_i\cdot(\vec{r}-\vec{r}_i)}e^{-i\vec{k}_i\cdot\vec{r}_i}/r_i. \end{aligned} \tag{3.31}$$

The matrix element of this plane wave with the $T$ matrix gives rise to $-2\pi f(\pi)$. The total result is then

$$P(\hat{k}) = D|M|^2|\hat{\epsilon}\cdot\hat{k} + P_1 + P_2|^2, \tag{3.32}$$

where

$$P_1 = \sum_j (\hat{\epsilon}\cdot\hat{r}_j)e^{ikr_j(1-\cos\theta_j)}e^{-\gamma r_j + \gamma_z \vec{r}_j\cdot\hat{z}}\frac{f(\theta_j)}{r_j} \tag{3.33}$$

and

$$P_2 = \sum_j (\hat{\epsilon}\cdot\hat{r}_j)e^{i2kr_j}e^{-2\gamma r_j}\frac{f(\pi)f_c(\pi-\theta_j)}{r_j^2}. \tag{3.34}$$

In Eq. (3.33) $\vec{r}_j\cdot\hat{z} < 0$ and $\gamma_z$ is defined in Eq. (3.23). Interestingly enough if we examine the terms linear in $f$ and integrate over $\hat{k}$ the term $P_2$ produces a factor $i(e^{2i\delta_1'} - 1)f(\pi)e^{2ikr_j}/2kr_j^2$ by projecting out the $l=1$ component of $f_c(\pi-\theta)$. This term is just what is necessary to combine with the angular average of the $P_1$ term to reproduce the EXAFS result with the central atom phase shift. The term $P_2$ has a simple physical origin. It is simply the second-order process in which the photoelectron is backscattered by the neighbor [thus accounting for the $f(\pi)$] and is then scattered by the central atom into the $\hat{k}$ direction [with amplitude $f_c(\pi-\theta_j)$]. Thus the single scattering EXAFS theory actually includes multiple scattering contributions in angular resolved photoemission. We note that these multiple scattering terms are special in that they have an effective path length of $2kr_j$ whereas all other terms have longer path lengths.

Strictly speaking, the simple scattering theory is valid only to lowest order in $P_1$ and $P_2$ and for a polarization direction such that $\hat{\epsilon}\cdot\hat{k}$ is not too small, Eq. (3.32) should be expanded as follows:

$$P(\hat{k}) = D|M|^2[(\hat{\epsilon}\cdot\hat{k})^2 + 2(\hat{\epsilon}\cdot\hat{k})\mathrm{Re}(P_1+P_2)]. \tag{3.35}$$

This equation can be interpreted in the same way

as EXAFS except that in addition to oscillations with period $2r_j$, there are oscillations with period given by the sum of $r_j$ and the projection of $-\vec{r}_j$ to the normal to the surface plane. It is worth noting that the $P_1$ term is larger than the EXAFS oscillation given in Eq. (2.2) by a factor of $kr_j$ which also means that it converges more slowly in a sum over $r_j$. This interpretation is especially interesting for emission normal to the plane. For adatoms occupying reasonable bonding sites there is usually sufficient symmetry so that several substrate atoms have the same interference path lengths. In that case Eq. (3.35) suggests that Fourier-transform techniques may be applied to separate out these path lengths. In particular, the path length to the nearest neighbor is expected to be considerably shorter than either $2r_i$ or path lengths to other neighbors which means that it should be readily resolved. Another interesting observation is that the central atom phase shift does not enter into the $P_1$ term in Eq. (3.35). In EXAFS it is found that the $k$ dependence or the central atom phase shift dominates that of the phase of $f(\pi)$. This $k$ dependence introduces shifts in the absolute position determination that necessitates corrections by the use of empirical standards.[18] Such corrections are unnecessary here for distances that appear in $P_1$. We should caution, however, that the phase of $f(\theta_j)$ may have stronger dependence on $k$ than the phase of $f(\pi)$.

It remains to discuss the importance of multiple scattering. Multiple scattering can be included in our short-range-order theory by adding more and more complicated paths. Just as in EXAFS each multiple scattering path can be characterized by its interference path length which is equal to

$$r_{ij\cdots kl} = r_i + |\vec{r}_i - \vec{r}_j| + \cdots + |\vec{r}_k - \vec{r}_l| - \hat{k}\cdot\vec{r}_l .$$

There are two separate questions one can raise: (i) is Fourier transform still a viable technique, and (ii) how important are the multiple scattering corrections to $P(\hat{k})$? If $\hat{k}$ is normal to the surface plane multiple scattering corrections to $P_1$ and $P_2$ involve long interference path lengths. It should be possible to separate these from the single scattering path lengths by Fourier transform. However, unlike EXAFS, there exist contributions to $P(\hat{k})$ that involve difference in path lengths arising from $(P_1+P_2)*(P_1+P_2)$. For Fourier transform to be useful we must require that such terms are small, i.e., $|P_1|$ and $|P_2|$ must be much less than unity. This will probably be the case for relatively high photoelectron energy when both the scattering amplitude and the Debye-Waller factor tend to reduce $P_1$ and $P_2$. As far as the importance of multiple scattering is concerned, the case of normal emission is more closely analogous to EXAFS and we might argue that multiple scattering paths are long and make rapidly oscillating contributions to $P_1$ and $P_2$ which tend to average to zero. The importance of multiple scattering clearly depends on the electron mean free path and our argument needs to be supported by detailed calculation or by comparison with experiment. Recently Liebsch[13] has calculated the multiple scattering contribution for an overlayer of sulphur on nickel. His results show that the modulation amplitudes are large and that multiple scattering is very important even for normal emission. While the inclusion of thermal vibration may reduce both the amplitude and the importance of multiple scattering and the situation may also change for heavier substrates that have larger damping coefficients or for more open substrate structures like those appropriate for semiconductors, at this stage it appears that full multiple scattering calculations have to be performed to analyze photoemission data.

## IV. CONCLUSION

Final-state interference effects can be used as a basis of powerful new techniques for determination of adsorbate structure. Observation of the Auger spectral lines is a way of measuring EXAFS from adatoms. Our calculations indicate that EXAFS is sensitive to the symmetry and the bond length of the adsorbed atom. We also elucidate the connection between EXAFS and angular resolved photoemission and conclude that measurement of the intensity of electrons emitted outside the crystal is not equivalent to EXAFS. The theory for the special case of emission normal to the surface is very similar to EXAFS theory which suggests that it may be possible to determine bond lengths directly by Fourier transform if data over a sufficiently wide energy range ($\approx$1000 eV) are available. If these suggestions turn out to be true, analysis of the data will be very simple. Otherwise LEED-type calculations have to be performed and compared with experiment. While the theoretical simplicity is lost, photoemission measurement will still be a valuable tool when compared with LEED as LEED is sensitive to the adsorbate and substrate together whereas the signal from photoemission originates only from the adsorbate.

## ACKNOWLEDGMENTS

I have benefited greatly from discussions with P. Citrin throughout the course of this work. I also thank G. Beni for discussions, particularly on the incoming and outgoing modifications of the final state.

[1]D. E. Sayers, F. W. Lytle, and E. A. Stern, Phys. Rev. Lett. 27, 204 (1971); E. A. Stern, D. E. Sayers, and F. W. Lytle, Phys. Rev. B 11, 4836 (1975).
[2]B. M. Kincaid and P. Eisenberger, Phys. Rev. Lett. 34, 1361 (1975).
[3]P. A. Lee and J. B. Pendry, Phys. Rev. B 11, 2795 (1975).
[4]C. A. Ashley and S. Doniach, Phys. Rev. B 11, 1279 (1975).
[5]J. Jaklevic, J. A. Kirby, M. P. Klein, A. S. Robertson, G. Brown, and P. Eisenberger (unpublished).
[6]H. Petersen and C. Kunz, Phys. Rev. Lett. 35, 863 (1975).
[7]S. Kikuchi, Proc. Jpn. Acad. 4, 271 (1928); 4, 275 (1928); 4, 354 (1928); 4, 475 (1928).
[8]M. von Laue, Ann. Phys. (Paris) 23, 705 (1935); see R. W. James, *The Optical Principles of the Diffraction of X-Ray* (Bell, London, 1962), p. 455.
[9]A. Liebsch, Phys. Rev. Lett. 32, 1203 (1974).
[10]L. McDonnell, D. P. Woodruff, and B. W. Holland, Surf. Sci. 51, 249 (1975).
[11]J. B. Pendry, J. Phys. C 8, 2418 (1975).
[12]B. W. Holland, J. Phys. C 8, 2679 (1975).
[13]A. Liebsch, Phys. Rev. B 13, 544 (1976).
[14]J. B. Pendry, *Low Energy Electron Diffraction* (Academic, New York, 1974).
[15]S. Y. Tong, in *Progress in Surface Science*, edited by S. G. Davison (Pergamon, New York, 1975), Vol. 7.
[16]P. A. Lee (unpublished).
[17]J. E. Demuth, D. W. Jepsen, and P. M. Marcus, Phys. Rev. Lett. 31, 540 (1973); 32, 1182 (1974).
[18]P. H. Citrin, P. Eisenberger, and B. M. Kincaid (unpublished).
[19]G. Beni, P. A. Lee, and P. M. Platzman, Bull. Am. Phys. Soc. 20, 488 (1975); Phys. Rev. B 13, 5170 (1976); P. A. Lee and G. Beni, Bull. Am. Phys. Soc. 21, 310 (1976).
[20]P. M. Marcus (private communication).
[21]For a review of the $T$-matrix formalism see P. Lloyd and P. V. Smith, Adv. Phys. 21, 69 (1972).
[22]G. Breit and H. Bethe, Phys. Rev. 93, 888 (1954); see also L. Schiff, *Quantum Mechanics*, 2nd ed. (McGraw-Hill, New York, 1955), p. 274.
[23]H. S. W. Massey, *Electronic and Ionic Impact Phenomena* (Oxford, 1969), p. 692.
[24]This is the form that corresponds to spherical harmonics decomposition of Eq. (3.27) and is convenient for our purpose because of our choice on the final state $|\vec{k}\rangle$ as a plane wave plus a spherical wave. Alternately, one can choose $\Phi_l$ to be real. The factor $e^{i\delta_l}$ will appear in Eq. (3.29), but then one has to be careful about the phase of the matrix element $M$ from the zeroeth-order term $\langle \vec{k}|\vec{r}|i\rangle$.